Experimental Procedures

Preparation of NMR samples

S5a (196-306) and K48-linked diubiquitin were produced as described (Pickart and Raasi, 2005; Raasi and Pickart, 2005; Varadan et al., 2002; Wang et al., 2003; Young et al., 1998). Briefly, we used recombinant monoubiquitin in which either an aspartic acid is added to the chain (Ub-D77) or the lysine at position 48 was mutated to an arginine (Ub-K48R). Using these two monoubiquitin samples, K48-linked diubiquitin could be synthesized. Ub-D77 and Ub-K48R that were selectively labeled or unlabeled were incubated with 0.1 μM UBE1 (E1, Boston Biochem), 25 μM UBE2K (E2), 2 mM ATP, and 1/5 total volume PBDM8 buffer at 37°C for ~12 hours. The diubiquitin formed was subsequently purified by using a monoQ column, followed by monoS ion-exchange columns (GE Healthcare). A similar procedure was used to produce K48-linked diubiquitin mutant with its proximal subunit MTSL labeled. In this case, however, a ubiquitin truncated mutant (Ub-G75C) with the C-terminal G75 substituted with cysteine was used.

His-tagged S5a (196-306) and GST-tagged hRpn13 (1-150) are expressed in *Escherichia coli* and purified by using a combination of affinity chromatography and size exclusion chromatography on an FPLC system. hRpn13 (1-150) is cleaved from its GST-tag during elution from glutathione S-sepharose resin by using PreScission protease (GE healthcare). ^{15}N, ^{13}C, and ^{2}H labeled samples are produced by growth in M9 minimal media with ^{15}N labeled ammonium chloride, ^{13}C labeled glucose, and D_2O used as the nitrogen, carbon, and water sources, respectively. Amide atoms are exchanged into D_2O when desired by using lyophilisation.

NMR spectroscopy

Chemical shift perturbation analysis was done by using $^{1}H,^{15}N$ HSQC experiments which were recorded on ^{15}N labeled S5a (196-306) with increasing molar ratios of unlabeled diubiquitin. Since UIM1 and UIM2 binding to diubiquitin was in the intermediate to slow exchange regime, the affected resonances could not be readily followed from their free to their bound states as increasing amounts of the binding partner was added. Therefore, an ^{15}N-dispersed NOESY spectrum recorded on ^{15}N labeled S5a (196-306) and unlabeled diubiquitin was used to obtain chemical shift assignments for diubiquitin-bound S5a (196-306). The concentration of S5a (196-306) for the $^{1}H,^{15}N$ HSQC titration and ^{15}N dispersed NOESY experiments was 0.40 mM. The spectra were recorded at 25°C and in Buffer 1 (20 mM $NaPO_4$, 100 mM NaCl, at pH 6.5).

Since many backbone HN groups belonging to UIM1 resonances were broadened beyond detection, a 3D ^{13}C-edited NOESY spectrum (100 ms mixing time) on ^{13}C-labeled S5a (196-306) mixed with 3-fold molar excess unlabeled diubiquitin was recorded to assign the diubiquitin-bound state of S5a. This molar ratio ensures that essentially all of S5a is diubiquitin-bound. Since sedimentation velocity analysis revealed a 1:1 binding stoichiometry for the S5a (196-306):diubiquitin complex, even with either component is at 7-fold molar excess (Figure 1D), we are able to use molar ratios greater than 1:1 to increase sensitivity by increasing the population of the bound state for the labeled protein. Unlike amide groups, the NMR resonances for aliphatic CH groups in proteins are less sensitive to dynamic motions and therefore those of UIM2, the internal helix, and part of UIM1 are observable in the recorded ^{13}C-edited NOESY spectrum (Supplementary Figure 2B).

Intermolecular NOE interactions between S5a (196-306) and K48-linked diubiquitin were obtained through four sets of NOESY experiments including ^{13}C-filtered, ^{13}C-edited NOESY spectra acquired ^{13}C-labeled S5a (196-306) mixed with 3-fold molar excess unlabeled diubiquitin, ^{13}C-labeled S5a (196-306) mixed with 3-fold molar excess diubiquitin with its proximal subunit 100% deuterated, diubiquitin with its proximal subunit ^{13}C labeled mixed with 2-fold molar excess unlabeled S5a (196-306), and diubiquitin with its distal subunit ^{13}C labeled mixed with 2-fold molar excess unlabeled S5a (196-306). In all spectra, the concentration of ^{13}C labeled protein was 0.4 - 0.5 mM and they were recorded at 25°C and on either 800 or 900 MHz spectrometers equipped with cryogenically cooled probes in Buffer 2 (20 mM $NaPO_4$, 50 mM NaCl, at pH 6.5). Whereas assignment of diubiquitin-bound S5a (196-306) resonances required the NOESY experiment described in the previous section, S5a-bound diubiquitin was straightforward to assign. Firstly, the chemical shift dispersion of ubiquitin is greater than S5a (196-306) and secondly, the chemical shift values for each subunit differed little from monoubiquitin's S5a-bound state. With the four half-filtered experiments, we readily assigned intermolecular NOEs, as NOEs between ^{13}C-labeled S5a and unlabeled ubiquitin were matched with though of ^{13}C labeled ubiquitin and unlabeled S5a. For example, the intermolecular NOE between K48's Cα proton from proximal ubiquitin and UIM2's M291's methyl protons was observed in S5a was ^{13}C labeled (Figure 2C) as well as when the proximal subunit of ubiquitin was ^{13}C labeled (Supplementary Figure 3A).

Chemical shift perturbation analysis was conducted by recording ^{1}H, ^{15}N HSQC or ^{1}H, ^{13}C HMQC experiments. Samples contained ^{15}N labeled Rpn13 (1-150), ^{13}C labeled S5a (196-306) and unlabeled diubiquitin or unlabeled Rpn13 (1-150), ^{13}C labeled S5a (196-306) and diubiquitin with one of its subunits ^{15}N labeled. The NMR spectra were

acquired at 0.3 mM and all mixtures were equimolar. Spectra were taken in Buffer 2 on a Varian Inova 800 MHz spectrometer with a cryogenically cooled probe.

Structure calculations

Structure calculations of the S5a (196-306):K48-linked diubiquitin complex were performed based on the NOE-derived distance and dihedral angle constraints. Intramolecular constraints for S5a (196-306) and those published for ubiquitin (PDB code 1D3Z) (Cornilescu et al., 1998) were incorporated to maintain the structure of each component, as neither protein undergoes gross structural change upon binding (see Results). The structure of the major binding mode was defined by 34 UIM2:proximal ubiquitin and 12 UIM1:distal ubiquitin intermolecular NOE derived distance restraints. The UIM2:distal interaction for the minor S5a:diubiquitin complex was defined by 24 intermolecular NOE derived distance restraints, which were still observable when the proximal subunit of diubiquitin was fully deuterated (Figure 2C red). Intermolecular NOEs between UIM1 and proximal ubiquitin were too weak to be observed and therefore the UIM1 constraints to distal ubiquitin were used to model the UIM1:proximal interaction. For both S5a:diubiquitin complexes, simulated annealing in XPLOR version 3.851 was performed on a Linux operating system. 30 randomly coiled structures were subjected to 15,000 simulated annealing and cooling steps of 0.005 ps to generate seven converged structures. These were selected because they have no NOE violation > 0.3 Å or dihedral angle violation > 10°. For the model demonstrating expected distances between MTSL and specific amide atoms of interest, the exact MTSL orientation is not known.

Gibbs free energy calculation

The Gibbs free energy required for a 3:1 population difference was determined by using Equations 1 and 2, in which R, T, and K are the gas constant (8.3145 $JK^{-1}mol^{-1}$), temperature of the NMR experiments (298K), and equilibrium constant, respectively.

$$\Delta G = -RT(\ln K_{major} - \ln K_{minor}) = -RT\ln(\frac{K_{major}}{K_{minor}}) \quad (1)$$

$$K_{major} = \frac{[(S5a:diUb)_{major}]}{[S5a][diUb]} \qquad K_{minor} = \frac{[(S5a:diUb)_{minor}]}{[S5a][diUb]} \quad (2)$$

Spin labeling experiments

The expression plasmids for the S5a (196-306) mutants and hRpn13 (1-150) CtoA mutant, in which all of its cysteines are mutated to alanine were made by using Quick Change Site Directed Mutagenesis Kit (Stratagene). S5a (196-306) Q227C and A298C mutants (His-tagged) and hRpn13 (1-150) CtoA mutant (GST-tagged) were expressed and purified from *Escherichia coli* by using a combination of affinity and size exclusion chromatography on an FPLC system, as described above for the wild-type proteins. Diubiquitin with G75 of its proximal subunit substituted with cysteine was also produced as described above. Purified diubiquitin-proximal G75C as well as S5a (196-306) Q227C and A298C proteins were spin labeled by reacting them with MTSL purchased from TRC (Toronto). Spin labeling reactions were performed in 50 mM Tris, pH 7.6, in a 10-fold excess of MTSL, and the reaction tubes were incubated in the dark at 4 °C overnight. Excess MTSL reagent was removed by extensive dialysis at 4 °C into NMR buffer (20 mM sodium phosphate, 50 mM sodium chloride, pH 6.5).

A series of $^{1}H,^{15}N$ HSQC experiments were recorded on 0.3 mM K48-linked diubiquitin with its proximal or distal subunits ^{15}N labeled without or with the addition of equimolar MTSL labeled S5a Q227C or A298C. $^{1}H,^{15}N$ HSQC experiments for protein samples of

K48-linked diubiquitin with its proximal or distal subunits ^{15}N labeled in the presence of equimolar hRpn13 (1-150) CtoA and MTSL labeled S5a Q227C or A298C were also acquired under identical conditions.

We also recorded a series of $^{1}H,^{15}N$ HSQC experiments on 0.3 mM ^{15}N labeled Rpn13 (1-150) CtoA protein without or with the addition of equimolar MTSL labeled diubiquitin G75C. These experiments were also done with equimolar S5a (196-306) present under identical conditions. For both the binary and ternary NMR samples, two HSQC experiments were acquired, one with MTSL in the oxidized state (paramagnetic state) and one with MTSL reduced to ensure effects were MTSL specific. The spin label quenching was achieved by addition of 5-fold molar excess ascorbic acid to the binary NMR sample (Rpn13 plus spin labeled diubiquitin G75C) and also the ternary NMR sample (Rpn13 plus spin labeled diubiquitin G75C and S5a (196-306)). Samples were placed in the magnet at 25 °C for 1 hour to ensure complete reduction of the spin label moiety.

References

Cornilescu, G., Marquardt, J.L., Ottiger, M., and Bax, A. (1998). Validation of Protein Structure from Anisotropic Carbonyl Chemical Shifts in a Dilute Liquid Crystalline Phase. J Am Chem Soc *120*, 6836-6837.

Pickart, C.M., and Raasi, S. (2005). Controlled synthesis of polyubiquitin chains. Methods Enzymol *399*, 21-36.

Raasi, S., and Pickart, C.M. (2005). Ubiquitin chain synthesis. Methods Mol Biol *301*, 47-55.

Varadan, R., Walker, O., Pickart, C., and Fushman, D. (2002). Structural properties of polyubiquitin chains in solution. J Mol Biol *324*, 637-647.

Wang, Q., Goh, A.M., Howley, P.M., and Walters, K.J. (2003). Ubiquitin recognition by the DNA repair protein hHR23a. Biochemistry *42*, 13529-13535.

Young, P., Deveraux, Q., Beal, R.E., Pickart, C.M., and Rechsteiner, M. (1998). Characterization of two polyubiquitin binding sites in the 26 S protease subunit 5a. J Biol Chem *273*, 5461-5467.

Supplementary Figures

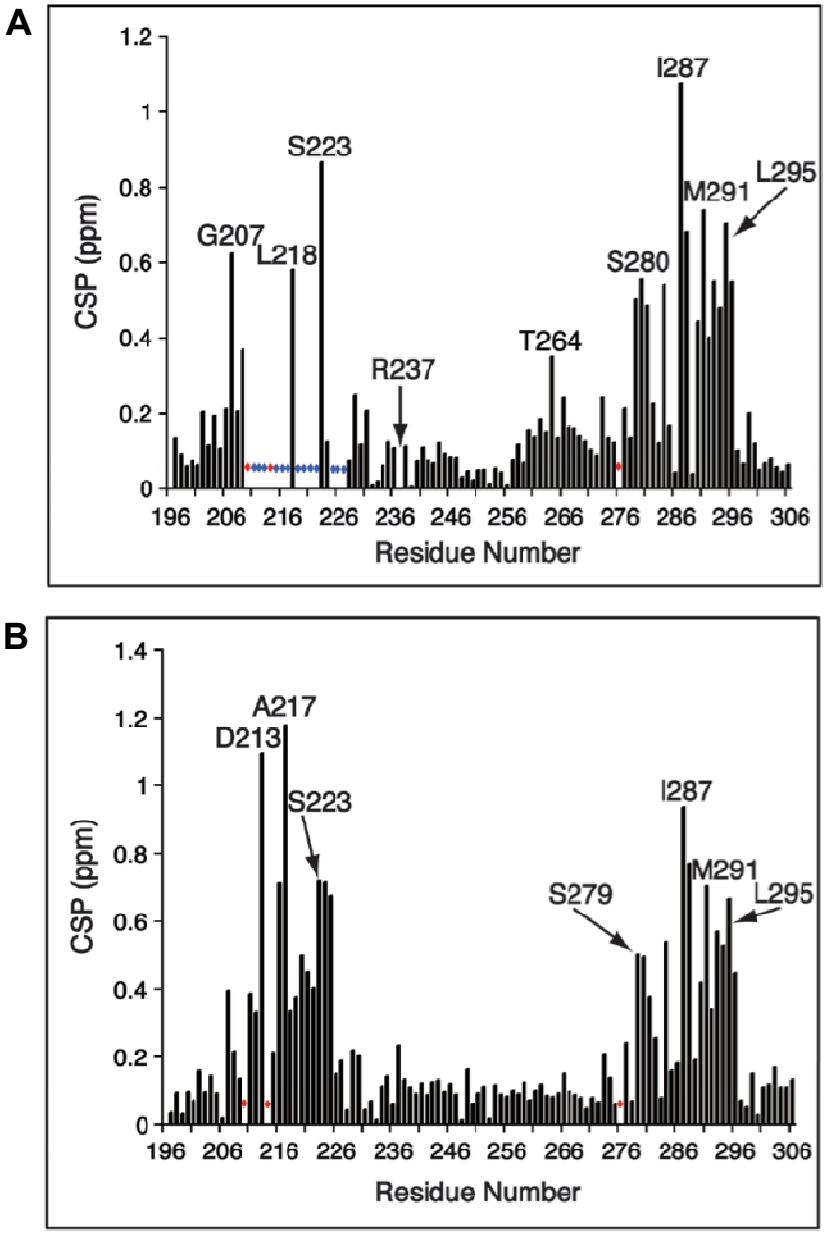

Supplementary Figure 1. Amide chemical shift perturbation experiments reveal new spectral changes for diubiquitin binding. A) Amide chemical shift perturbation analysis reveals the residues of S5a involved in binding diubiquitin. Residues that disappear upon diubiquitin binding and prolines, which lack amide protons, are labeled with blue and red stars, respectively. R237 of S5a could not be followed during the

titration series due to resonance overlap. B) Amide chemical shift perturbation analysis reveals the residues of S5a involved in binding monoubiquitin. Prolines are labeled with red stars. Chemical shift perturbation values ($\Delta\delta_{avg}$) for ^{15}N and ^{1}H nuclei were derived from $CSP=\sqrt{0.2\Delta\delta_N^2+\Delta\delta_H^2}$, where $\Delta\delta_N$ and $\Delta\delta_H$ represent the changes in the amide nitrogen and proton chemical shifts (in parts per million), respectively.

F) Supplemental Fig 2

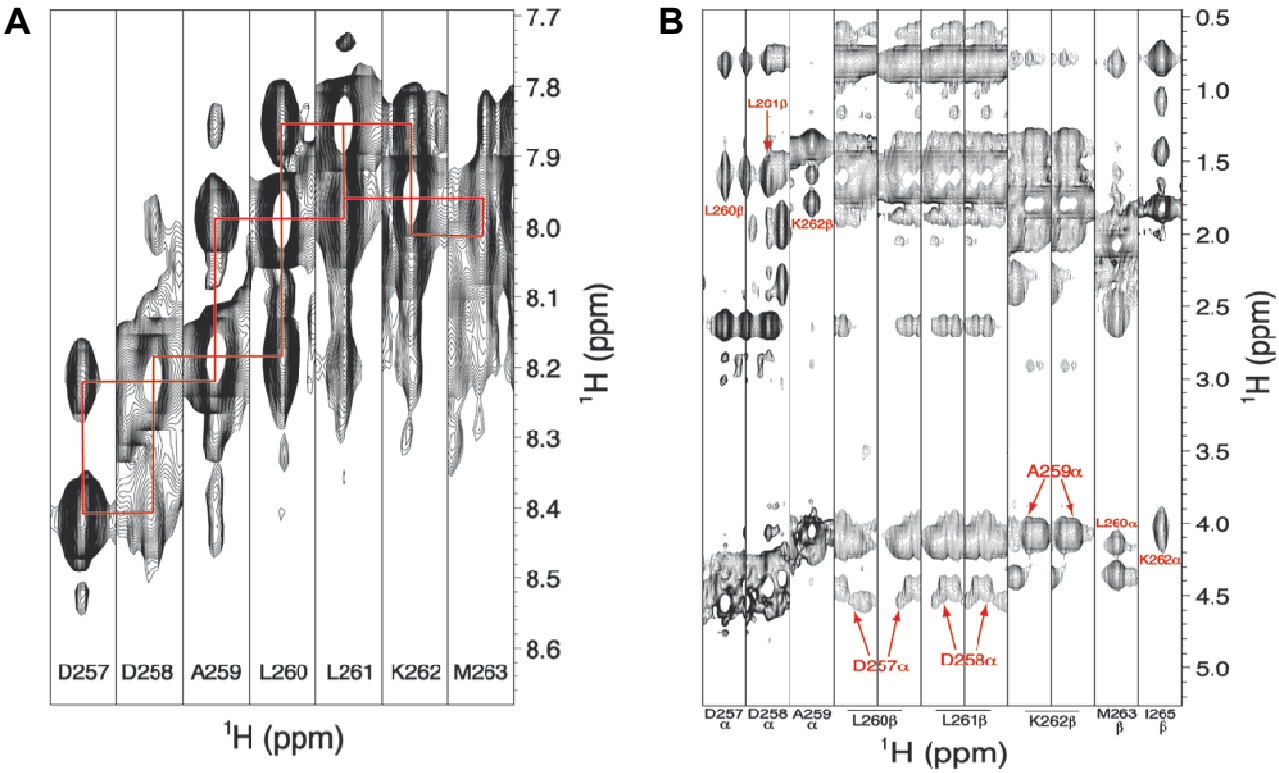

Supplementary Figure 2. S5a binding to diubiquitin does not disrupt the secondary structure of the helix between UIM1 and UIM2. A) An ^{15}N-dipersed NOESY spectrum recorded on ^{15}N-labeled S5a (196-306) and 3-fold molar excess unlabeled diubiquitin reveals strong amide-to-amide NOE crosspeaks, which are a signature for helices. B) A ^{13}C-dipersed NOESY spectrum recorded on ^{13}C-labeled S5a (196-306) and 3-fold molar excess unlabeled diubiquitin reveals NOE crosspeaks between Hα (i) and Hβ (i+3) atoms, which are a hallmark of helices.

F) Supplemental Fig 3

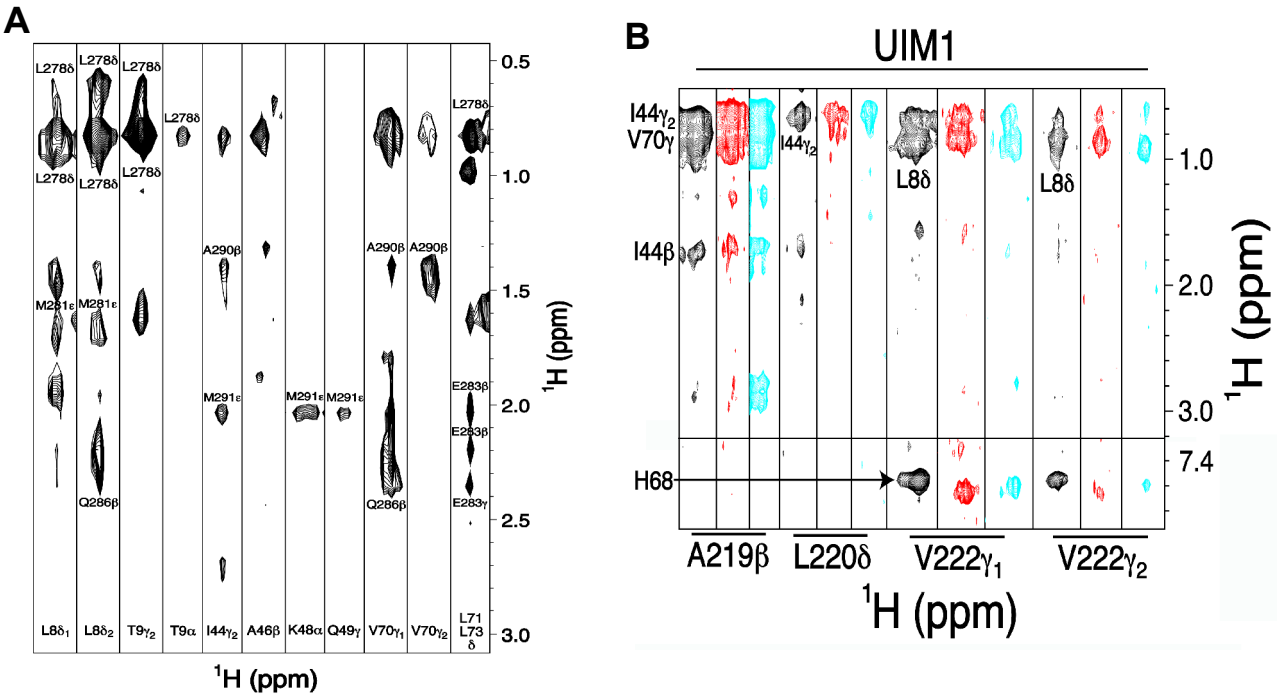

Supplementary Figure 3. UIM2 binds the proximal subunit while UIM1 binds the distal one. A) Abundant intermolecular interactions appear between UIM2 and K48-linked diubiquitin's proximal subunit. The spectrum of Figure 2A displayed in black, which contains NOEs between S5a and the proximal subunit of diubiquitin, is expanded to illustrate abundant NOE interactions. Intermolecular NOEs between S5a and proximal K48 reveal that S5a has contacts with the atoms connecting the two ubiquitin subunits. (B) Selected regions of experiments containing intermolecular NOE interactions between UIM1 of S5a (196-306) and diubiquitin (black and red) or monoubiquitin (light blue). ^{13}C half-filtered NOESY spectra recorded on ^{13}C-labeled S5a (196-306) mixed with 3-fold molar excess unlabeled K48-linked diubiquitin (black) or K48-linked diubiquitin with its proximal subunit deuterated (red) indicates the interactions to be unaffected by deuterating the proximal subunit. The binding pattern between UIM1 and diubiquitin mimics that with monoubiquitin, which is demonstrated by analogous intermolecular NOEs (light blue).

F) Supplemental Fig 4-8

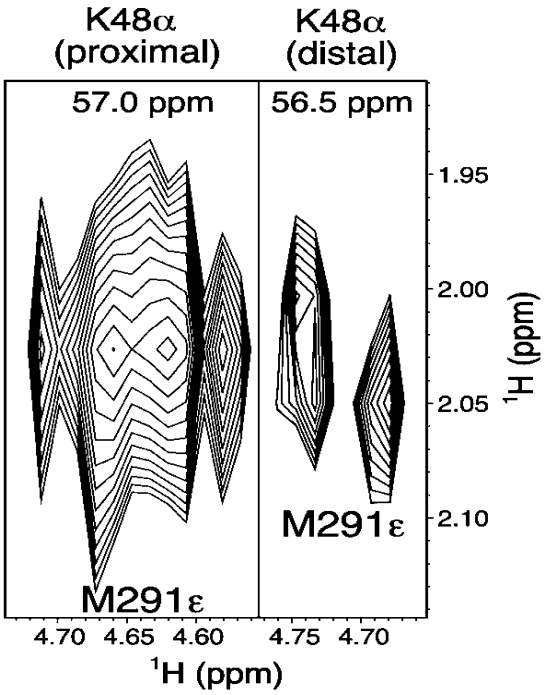

Supplementary Figure 4. The population of S5a's UIM2 bound to K48-linked diubiquitin's proximal subunit is in 3-fold molar excess over that bound to the distal one. ^{13}C half-filtered experiments were recorded in an identical manner on K48-linked diubiquitin with either its proximal (left) or distal (right) subunit ^{13}C labeled and mixed with unlabeled S5a (196-306). Intermolecular NOE interactions between M291's sidechain methyl group and proximal (left) or distal (right) K48's Hα proton were integrated to reveal population differences. Both experiments were performed with diubiquitin at 0.5 mM and S5a at 2-fold molar excess.

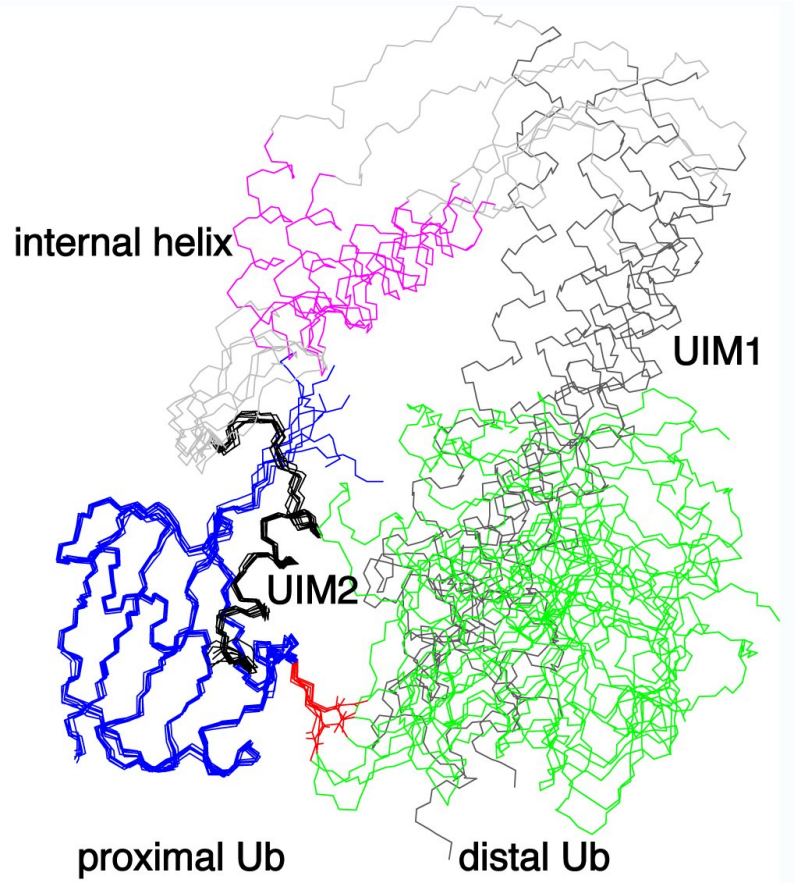

Supplementary Figure 5. Although significantly more restricted than when bound to monoubiquitin, S5a's UIMs retain some freedom in their relative positions due to the flexibility of the diubiquitin's linker region. The S5a (196-306):K48-linked diubiquitin structures with no NOE violation above 0.3 Å are displayed with the backbone heavy atoms of proximal ubiquitin and UIM2 superimposed. 7 structures are displayed from 30 randomly coiled starting structures. UIM1, the internal helix, and UIM2 of S5a are colored in dark grey, purple and black, respectively, whereas diubiquitin's distal and proximal subunits are highlighted in green and blue, respectively. The linker residues of diubiquitin (proximal K48 and distal G76) are highlighted in red.

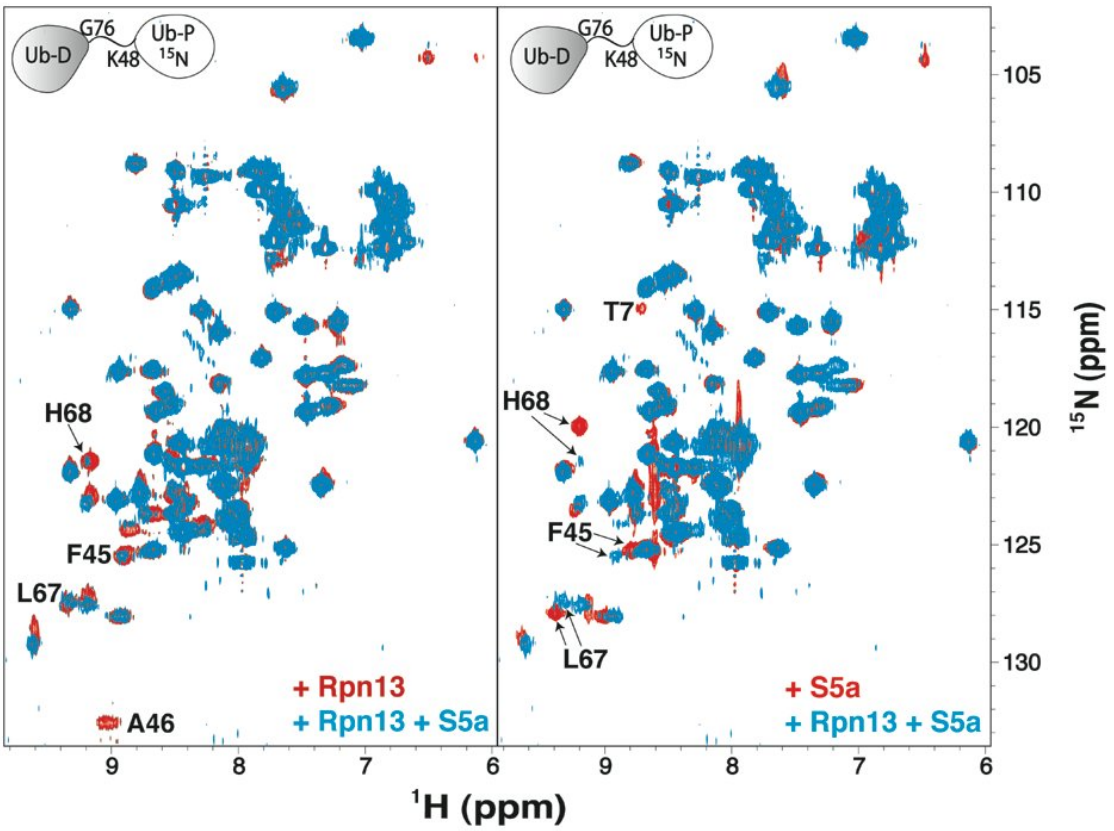

Supplementary Figure 6. Diubiquitin's proximal subunit binds predominately to Rpn13. ^{1}H,^{15}N HSQC spectra of K48-linked diubiquitin with its proximal subunit ^{15}N labeled in the presence of equimolar Rpn13 (left, red), S5a (right, red), or both of these ubiquitin receptors (blue). Selected ubiquitin resonances are labeled, including T7, F45, L67, and H68, which shift in a manner that reflects Rpn13 binding. Attenuation of A46 and H68 in the presence of Rpn13 and S5a suggests that, although a large fraction of the proximal subunit is bound to Rpn13, some minor exchange most likely occurs.

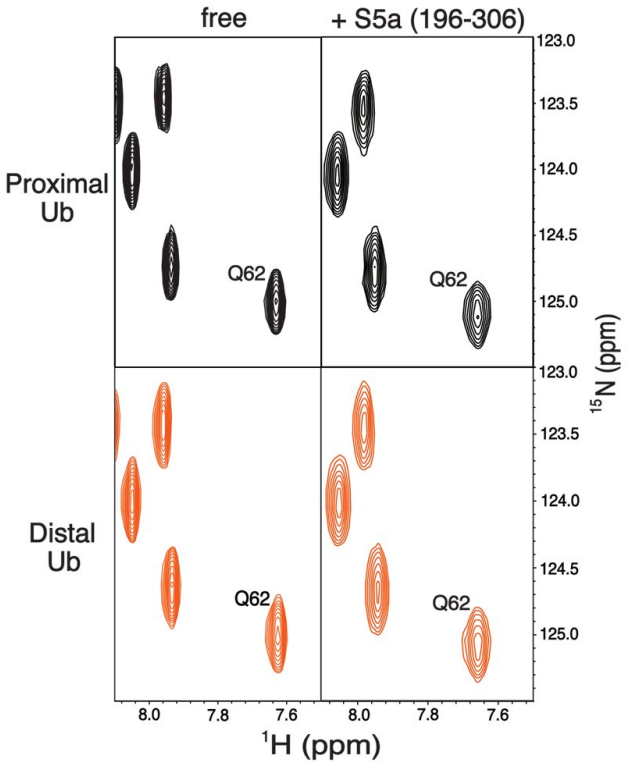

Supplementary Figure 7. Q62 of diubiquitin's proximal and distal subunits is not attenuated upon addition of unlabeled S5a (196-306). Expanded view of ^{1}H, ^{15}N HSQC spectra for the proximal (top panels) or distal (bottom panels) subunit of K48-linked diubiquitin alone (left panel), or with added unlabeled S5a (196-306) (right panel).

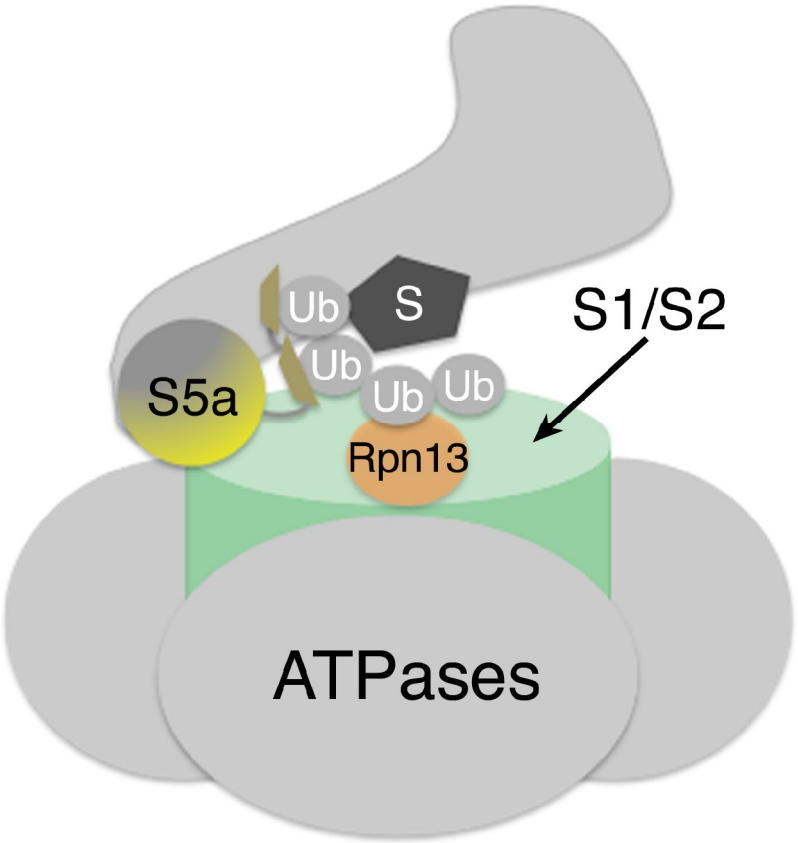

Supplementary Figure 8. Proposed model of Rpn13 and S5a binding simultaneously to a ubiquitinated substrate in the proteasome. Rpn13's ubiquitin-binding domain and S5a's N-terminal VWA domain are displayed bound to the S1 and S2 scaffolding proteins of the proteasome's regulatory particle as their ubiquitin-binding regions bind ubiquitin subunits of a ubiquitinated substrate. This coordinated binding may serve to properly orient the ubiquitin chain for subsequent processing by deubiquitinating enzymes in the proteasome.